Cold collisions in an atomic beam

H. R. Thorsheim, Y. Wang, and J. Weiner
Department of Chemistry and Biochemistry, University of Maryland, College Park, Maryland 20742
(Received 10 August 1989)

We report a measurement of the rate constant for associative ionization (AI) between excited Na(3*p*) atoms colliding within a single beam at a velocity of 11.9 $msec^{-1}$, corresponding to a temperature of 65 mK. The collisions take place in a narrow velocity class of excited atoms produced by crossing the collimated Na beam with a monomode dye laser at an angle of 45°. Light polarized linearly in the collision plane yields an AI rate constant greater than that for circular polarization by a factor of 2. We find $K^{\rm lin}_{65\,mK}=(12.2\pm4.3)\times10^{-13}$ $cm^3\,sec^{-1}$ and $K^{\rm cir}_{65\,mK}=(6.1\pm1.8)\times10^{-13}$ $cm^3\,sec^{-1}$. The experimental arrangement also permits absolute calibration of earlier crossed-beam measurements of the excitation function (cross section versus velocity) at conventional thermal beam kinetic energies. Present results together with earlier work show that the cross-sectional temperature dependence is in qualitative accord with theory.

The study of collision dynamics at kinetic energies corresponding to temperatures below 1 K promises to open a rich field of new phenomena in which alignment, orientation, and optical field play dominant roles. Cooling and trapping of atoms to submillikelvin temperatures by laser light[1] has permitted exploration of a regime where spontaneous emission is rapid compared to collision time, and where the deBroglie wavelength is longer than the range of the chemical bond by more than one order of magnitude. Several experimental reports have recently appeared in the literature[2–4] which indicate that very large cross sections and strong field-dressing effects[5,6] generally can be expected to figure importantly in inelastic processes.

Although "optical molasses" (see Ref. 1) and traps have successfully attained ensembles of ultracold atoms, for the purpose of studying collisions they suffer from the same disadvantage as conventional gas-bulb experiments—loss of well-defined spatial and polarization axes. We report here a beam technique that preserves this directionality, producing cold (65 mK) collisions between Na(3*p*) atoms, by restricting the distribution to a narrow velocity class excited by a single-mode laser. This technique does not produce the submillikelvin collision temperatures obtainable from optical traps, but kT nevertheless diminishes to values comparable to weak long-range interaction potentials which therefore control the final outcome of the collisional encounter. The beam environment preserves a reference for internuclear and excited-state polarization axes, useful for a detailed probe of the collisional process. As in Ref. 2, the collision is associative ionization (AI),

$$\mathrm{Na}(^2P_{3/2})+\mathrm{Na}(^2P_{3/2})\rightarrow \mathrm{Na}_2^{+}+e\ . \qquad (1)$$

We measure the rate constant for process (1) at 65 mK as a function of initial polarization and discuss the results in light of earlier ultracold results (Ref. 2), earlier crossed-beam measurements,[7] and recent theory.[8]

Figure 1 shows a diagram of the experiment. Two atomic beam sources are mounted in a vacuum chamber at right angles while two counterpropagating laser beams traverse the collision region diagonally with respect to the atomic beam axes. For the cold-collision measurements, atomic source 2 is flagged off; and ion signals from process (1) come only from intrabeam collisions within the selected velocity group of beam 1. A particle multi-

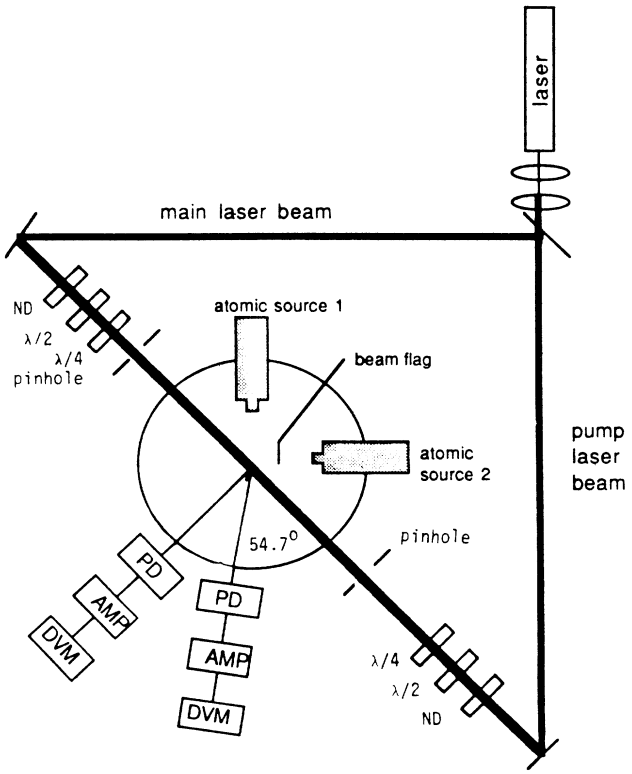

FIG. 1. Schematic diagram of the apparatus. Beam flag stops source 2 during single-beam experiments. PD, photodiodes; Amp, amplifiers; DVM, digital volt meters; ND, neutral density filters; λ/2, half-wave plates; λ/4, quarter-wave plates.

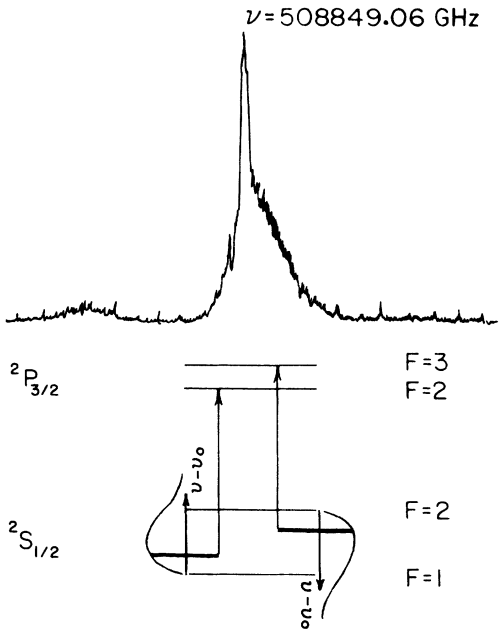

FIG. 2. Spectral profile of ion production showing the point at which a single frequency corresponding to a single velocity group excites two different different transitions with opposite Doppler shifts.

plier mounted above the interaction plane detects the ion production rate, and photodiodes fixed at 90° and 54.7° with respect to the quantization axis monitor excited-state fluorescence. Various combinations of quarter- and half-wave plates, and neutral density filters control laser polarization and intensity. Before entering the interaction region, a beam-expanding telescope increases the laser spot diameter to about 1 cm, and a 3.6-mm-diam pinhole then selects the central portion of uniform intensity before passing it into the collision apparatus. The two counterpropagating laser beams are tuned such that the frequency is resonant with the Doppler blue-shifted ν_{23}, $^2S_{1/2}(F=2)\rightarrow{}^2P_{3/2}(F=3)$, Na atomic hyperfine transition in one direction while resonant with the Doppler red-shifted ν_{12}, $^2S_{1/2}(F=1)\rightarrow{}^2P_{3/2}(F=2)$, transition in the other. As pointed out long ago,[9] this two-level, single-frequency technique maximizes excited-state population and avoids intensity-dependent optical pumping effects endemic to linearly polarized excitation. Once the laser-atomic beam angle θ is fixed, the relation that uniquely determines laser frequency ν_L and excited velocity group v is

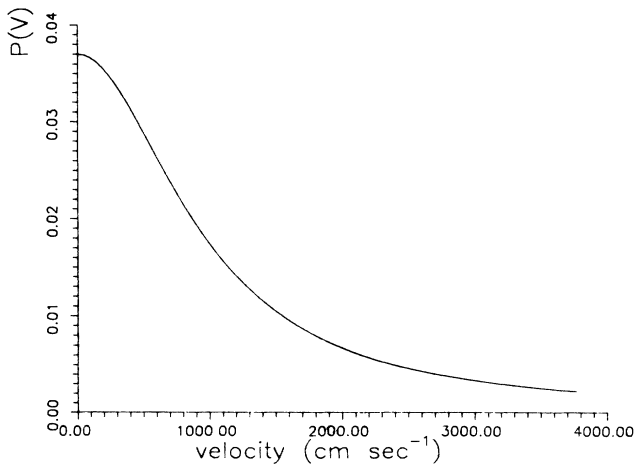

FIG. 3. Relative collision velocity distribution (normalized) within the excited velocity class in the atomic beam. The upper limit of the autocorrelation [see Eq. (3)] corresponds to the velocity above which the rate of photon absorption in the atomic beam is less than 0.01 of the rate at line center.

$$\nu_L[1+v/c\cos(\theta)]=\nu_{23}\ , \tag{2a}$$

$$\nu_L[1-v/c\cos(\theta)]=\nu_{12}\ . \tag{2b}$$

Figure 2 illustrates a spectral scan over the Doppler profile of atomic beam 1. The sharp peak at $\nu_L=508\,849.06$ GHz, satisfying Eqs. (2), corresponds to a velocity group peaked at 713 msec^{-1}. Either the laser linewidth or the natural linewidth of the atomic transition (whichever is larger) determines the distribution of relative collision speeds along the atomic beam axis. In the case of the Na resonance transition the natural width is 10 MHz, about an order of magnitude greater than the laser line. The distribution of axial collision speeds V_A is given by

$$P(V_A)=\int_{-\infty}^{+\infty}dv_2\int_{-\infty}^{+\infty}dv_1P_1(v_1)P_2(v_2)\times\delta(|v_1-v_2|-V_A)\ , \tag{3}$$

where $P_1(v_1)$ and $P_2(v_2)$ are the probabilities of exciting atoms 1 and 2, respectively,

$$P_i(v_i)=\frac{1}{2\pi}\frac{\Gamma_\nu(\lambda_0/\cos\theta)dv_i}{(v_i-v_0)^2+\Gamma_\nu^2/4(\lambda_0/\cos\theta)^2}\ ,\quad i=1,2 \tag{4}$$

where Γ_ν is the width of the atomic transition (Hz), and λ_0 the transition wavelength with the atom at rest. Figure 2 shows that $P(V_A)$ is the positive half of a Lorentzian function with full width 2Γ, arising from the correla-

TABLE I. Rate constants and absolute cross sections for associative ionization.

Rate constant [(cm^3 sec^{-1})$\times10^{13}$]	Cross section (cm$^2\times10^{17}$)	Temperature	Polarization	Reference
$110.0^{-50.0}_{+130.0}$	$86\,000.0^{-3500.0}_{+10\,000.0}$	0.75 mK	Mixed	2
6.1±1.8	48.6±20.0	73 mK	Circular	This work
12.2±4.3	97.2±45.0	73 mK	Linear	This work
17.0±6.0	1.69±0.6	472 K	Circular	This work
68.0±24.0	6.74±2.4	472 K	Linear	This work
68.0±25.0	5.7±2.1	~500 K	Linear	10
81.0±30.0	7.3±2.7	~600 K	Mixed	11

tion of two identical Lorentzians of width $\Gamma = \Gamma_v(\lambda_0/\cos\theta)$. Transverse velocity components V_T contribute from the atomic beam divergence (6 mrad), and the average collision velocity $\langle V_C \rangle$ is given by

$$\langle V_C \rangle = [\langle V_A \rangle + 2\langle V_T \rangle^2]^{1/2} . \quad (5)$$

With the excitation laser power at 1.7 mW cm^{-2}, the power-broadened transition width Γ_v is 11.3 MHz, and $\langle V_c \rangle = 11.9$ msec^{-1}. Laser beam absorption by the atomic beam determines the excited state density through the relation

$$I_0 - I = \frac{\mathrm{Na}^* A}{V} \hbar\omega F(\omega) x_0 , \quad (6)$$

where $I_0 - I$ is the absorbed intensity, Na* the number of excited atoms, V the defined volume of the laser-atom beam interaction, x_0 the atomic beam width, and A, $\hbar\omega$, and $F(\omega)$ the spontaneous emission rate, photon energy, and line-shape factor, respectively. Typically, Na* is about 5×10^6 resulting in an excited-state density n_{ex} of 10^8 cm^{-3}. The photodiode signals (see Fig. 1) are calibrated to the absorption measurement and monitor the excited-stated density during the course of the experiment. From the measured ion production rate N_{ion} (ions sec^{-1}), the number of excited atoms Na*, and the excited-state density n_{ex} we calculate the rate constant using the standard definitions

$$K = \langle \sigma V_c \rangle = N_{ion}/\mathrm{Na}^* n_{ex} . \quad (7)$$

Although the signal rate N_{ion}, rate constant K, and average cross section $\langle \sigma \rangle$ are directly related to the collision velocity $\langle V_c \rangle$ by Eq. (7), we label the measurement by a "temperature" defined as $T = \mu\langle V_c \rangle^2/3k_B$ so as to compare with previous experiments and theory (Refs. 2, 6, and 8). The result for circular polarization is $K^{cir}_{65\ mK} = (6.1\pm1.8)\times10^{-13}$ cm^3 sec^{-1} and for linear polarization $K^{lin}_{65\ mK} = (12.2\pm4.3)\times10^{-13}$ cm^3 sec^{-1}. Uncertainty in the excited-state volume (estimated at 20%) contributes the largest source of error. Corresponding cross sections $\langle \sigma \rangle = K/\langle V_c \rangle$ are $\langle \sigma \rangle^{cir}_{65\ mK} = (5.1\pm2.0)\times10^{-16}$ cm^2 and $\langle \sigma \rangle^{lin}_{65\ mK} = (10.2\pm4.5)\times10^{-16}$ cm^2.

If the second atomic beam is unblocked, the setup permits a direct measurement of the ratio of rate constants at 65 mK and 472 K (the temperature corresponding to the crossed-beam relative collision velocity). We calculate the absolute rate constants at 472 K from these ratios together with the absolute values at 65 mK. The results, $K^{cir}_{472\ K} = (1.7\pm0.6)\times10^{-12}$ cm^3 sec^{-1} and $K^{lin}_{472\ K} = (6.8\pm2.4)\times10^{-12}$ cm^3 sec^{-1}, calibrate earlier relative cross-sectional measurements (Ref. 7) to the same absolute scale. Table I summarizes rate constant measurements for process (1) spanning six orders of magnitude in collision energy. The absolute cross sections are plotted in Fig. 4 along with the results of a recent semiclassical calculation (Ref. 8).

The theoretical curve shows a decline in cross section with decreasing temperature until a minimum is reached around 70 K. The dropping cross section reflects the closing of molecular entrance channels as the collision kinetic energy falls below the minimum necessary to surmount long-range repulsive barriers. In the case of two Na(3p) atoms, the leading long-range electrostatic term in the interatomic potential is the quadrupole-quadrupole interaction which varies as C_5/R^5. Relative orientation of the two quadrupoles determines the sign of C_5, and

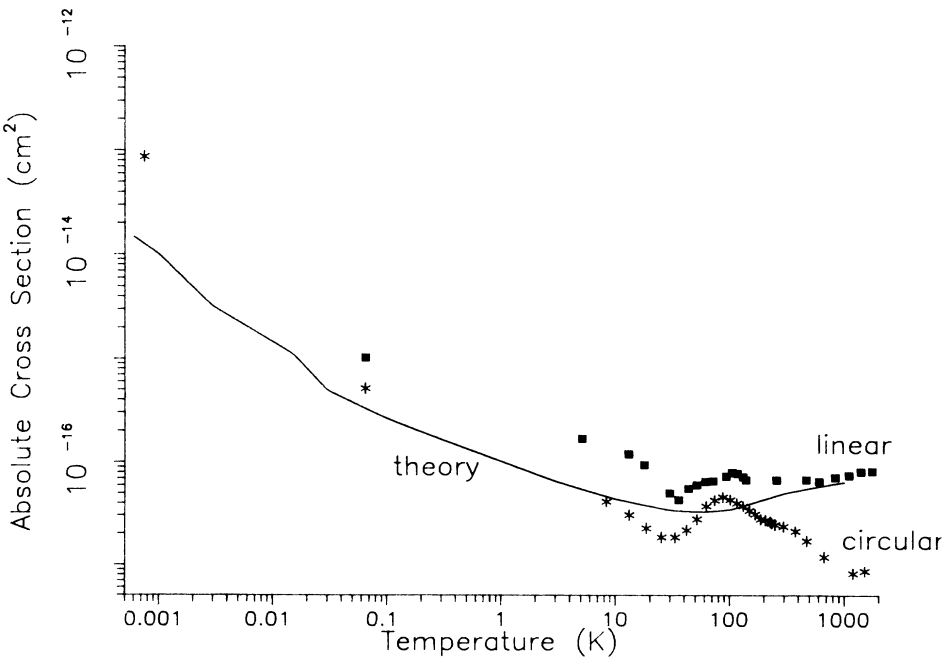

FIG. 4. Absolute cross section for associative ionization plotted against temperature. Present single-beam results are shown at 0.065 K. Higher temperature results are rescaled from Ref. 7 using present crossed-beam data (see discussion). Asterisks are circular polarization; closed squares are linear polarization.

only those orientations leading to molecular Π states exhibit attractive character. At kinetic energies lower than the minimum in the excitation function, cross sections begin to increase because the surviving entrance channels are radially attractive while angular momentum barriers continue to decrease. The number of partial waves contributing to the scattering event becomes severely restricted, and a fully quantal theory must take over from the semiclassical picture. Although the experimental points are in qualitative agreement with the calculated curve, the model leaves many unanswered questions. For example, important features such as hyperfine structure and the influence of optical field dressing on molecular states (see Refs. 5 and 6) at submillikelvin temperatures as well as the fine structure, and polarization dependence of the cross sections at higher temperatures require more extensive theoretical treatment. Furthermore, the curve in the vicinity of the predicted cross-section minimum has not yet been tested experimentally. It is to be expected that rapid technical development will permit beam experiments to expand into this presently inaccessible region, yielding important new insights into the transition zone from conventional to ultracold heavy-particle collision dynamics.

Support from the National Science Foundation through Grant No. PHY-8814361 and the University of Maryland Computation Center are gratefully acknowledged.

[1]For an early review of the mechanical effects of light see the special issue, J. Opt. Soc. Am. B **2**, 11 (1985).

[2]P. L. Gould, P. D. Lett, P. S. Julienne, W. D. Phillips, H. R. Thorsheim, and J. Weiner, Phys. Rev. Lett. **60**, 788 (1988).

[3]M. Prentiss, A. Cable, J. E. Bjorkholm, S. Chu, E. L. Raab, and D. E. Pritchard, Opt. Lett. **13**, 452 (1988).

[4]D. Sesko, T. Walker, C. Monroe, A. Gallagher, and C. Wieman, Phys. Rev. Lett. **63**, 961 (1989).

[5]P. L. Gould, P. D. Lett, R. N. Watts, C. I. Westbrook, P. S. Julienne, W. D. Phillips, H. R. Thorsheim, and J. Weiner, At. Phys. **11**, 215 (1989); (unpublished).

[6]P. S. Julienne and F. H. Mies, J. Opt. Soc. Am. B **6**, 2257 (1989).

[7]M.-X. Wang, J. Keller, J. Boulmer, and J. Weiner, Phys. Rev. A **34**, 4497 (1986); **35**, 934 (1987).

[8]S. Geltman, J. Phys. B **21**, 1735 (1989); **22**, 2049 (1989).

[9]G. M. Carter, D. E. Pritchard, and T. W. Ducas, Appl. Phys. Lett. **27**, 498 (1975).

[10]R. Bonanno, J. Boulmer, and J. Weiner, Phys. Rev. A **28**, 604 (1983); Comments At. Mol. Phys. **16**, 109 (1985).

[11]J. Huennekens and A. Gallagher, Phys. Rev. A **28**, 1276 (1983).

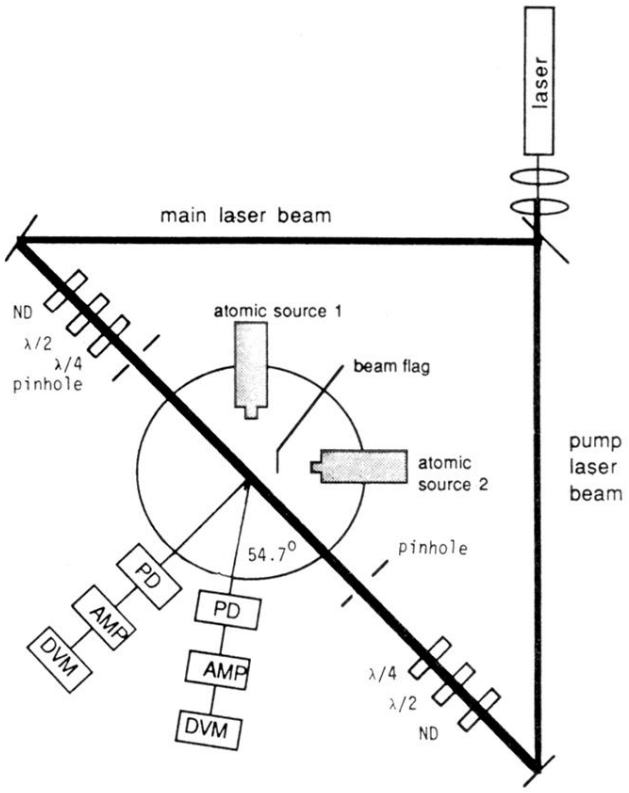

FIG. 1. Schematic diagram of the apparatus. Beam flag stops source 2 during single-beam experiments. PD, photodiodes; Amp, amplifiers; DVM, digital volt meters; ND, neutral density filters; $\lambda/2$, half-wave plates; $\lambda/4$, quarter-wave plates.